Article

# Direct Observation of Triplet State Emission of Single Molecules: Single Molecule Phosphorescence Quenching of Metalloporphyrin and Organometallic Complexes by Molecular Oxygen and Their Quenching Rate Distributions

Erwen Mei, Sergei Vinogradov, and Robin M. Hochstrasser

*J. Am. Chem. Soc.*, **2003**, 125 (43), 13198-13204• DOI: 10.1021/ja030271k • Publication Date (Web): 04 October 2003



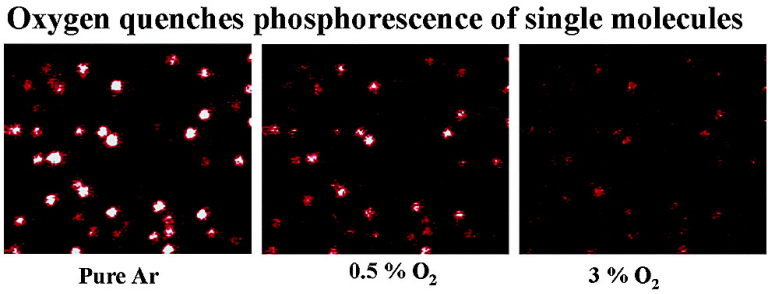


## More About This Article

Additional resources and features associated with this article are available within the HTML version:

- Supporting Information
- Links to the 5 articles that cite this article, as of the time of this article download
- Access to high resolution figures
- Links to articles and content related to this article
- Copyright permission to reproduce figures and/or text from this article

View the Full Text HTML

J|A|C|S
ARTICLES
Published on Web 10/04/2003

# Direct Observation of Triplet State Emission of Single Molecules: Single Molecule Phosphorescence Quenching of Metalloporphyrin and Organometallic Complexes by Molecular Oxygen and Their Quenching Rate Distributions

Erwen Mei,[†] Sergei Vinogradov,[‡] and Robin M. Hochstrasser*,[†]

*Contribution from the Department of Chemistry, and Department of Biochemistry and Biophysics, University of Pennsylvania, Philadelphia, Pennsylvania 19104*

Received May 1, 2003; E-mail: hochstra@sas.upenn.edu

***Abstract:*** Single molecules are detected through the phosphorescence emission of their triplet states. Emission of the triplet states of single molecules of Pt octabutoxycarbonyl porphyrin (PtOBCP) and ruthenium(II)-tris-4,7-diphenyl-1,10-phenanthroline dichloride ($Ru(dpp)_3Cl_2$) is reported. The single molecule phosphorescence is very sensitive to molecular oxygen. Each molecule has its own characteristic quenching rate by oxygen, and the distribution of these rates is measured for ($Ru(dpp)_3Cl_2$) on a quartz surface. The large variance of this distribution is presumed to be caused by fluctuations in the pseudobimolecular rate coefficient and the local oxygen concentration. The possibility of creating a quantitative single oxygen molecule sensor is suggested.

## Introduction

In recent years single molecule spectroscopy carried out at room temperature in fluids has opened new avenues for studying the heterogeneity presented by materials, macromolecules, and the dynamics of proteins and enzymes.[1−3] By probing chemical dynamics and kinetics at the single molecule level, one can obtain direct measurements of distributions of physical and chemical properties, which are difficult to glean from conventional ensemble experimental methods. A wide range of single molecule detection technologies based on different detection mechanisms has been explored.[4−7] Among them, single molecule spectroscopy based on fluorescence detection has proven to be powerful and effective. The advantages of using fluorescence for single molecule detection include high sensitivity and low noise, features that permit a broad range of applications in biological systems, for which the development and use of fluorescence probes is already at a very advanced stage. However, the fluorescence signal fluctuations might involve dynamical characteristics of several electronic states, such as the ground state, excited states, and triplet states,[8] any of which can undergo thermal or photochemical reactions. As a result, the intensity−time record of single molecule fluorescence is usually a response to many processes, not all of which are well understood.

The complexity of fluorescence processes endows single molecule fluorescence intensity−time records with some undesirable characteristics. For example, the fluorescence intensity signal is often observed to fluctuate on time scales that are not directly associated with the conventional photophysical processes, such as fluorescence, internal conversion, and intersystem crossing. These so-called "blinking" effects can interfere with the interpretation of single molecule fluorescence data, especially in biological systems, such as proteins and enzymes, whose dynamics also can cause fluctuations of the fluorescence signal on similar time scales.[2,9] Single molecule fluorescence intensity fluctuations can arise from a number of sources such as changes in the orientation of the molecular transition dipole axis that affects the efficiency of absorption, intersystem crossing to a long-lived triplet state that introduces intermittency into the fluorescence time record, spontaneous or light-induced spectral shifts which result in changes in the absorption cross section at the excitation frequency, or spontaneous and light-induced chemical changes that alter the emission yield. The intermittent behavior of single molecule fluorescence signals has been extensively studied by several groups,[10,11] but, so far, a detailed generally applicable mechanism has not been established. Also, the role of triplet states in these processes as well as in photobleaching is not often obvious from the measurement of single molecule signals. It therefore seems of some value to

[†] Department of Chemistry.
[‡] Department of Biochemistry and Biophysics.

(1) Moerner, W. E.; Orrit, M. *Science* **1999**, *283*, 1670−1675.
(2) Lu, H. P.; Xun, L.; Xie, S. X. *Science* **1998**, *282*, 1877−1882.
(3) Weiss, S. *Science* **1999**, *283*, 1676−1683.
(4) Nie, S. M.; Emery, S. R. *Science* **1997**, *275*, 1102−1106.
(5) Ambrose, W. P.; Moerner, W. E. *Nature* **1991**, *349*, 225−227.
(6) Ambrose, W. P.; Goodwin, P. M.; Martin, J. C.; Keller, R. A. *Phys. Rev. Lett.* **1994**, *72*, 160−163.
(7) Carrion-Vazquez, M.; Oberhauser, A. F.; Fisher, T. E.; Marszalek, P. E.; Li, H.; Fernandez, J. M. *Prog. Biophys. Mol. Biol.* **2000**, *74*, 63−91.
(8) Lakowicz, J. R. *Principles of Fluorescence Spectroscopy*, 2nd ed.; Kluwer Academic: New York, 1999.
(9) Jia, Y.; Talaga, D. S.; Lau, W. L.; Lu, H. S. M.; DeGrado, W. F.; Hochstrasser, R. M. *Chem. Phys.* **1999**, *247*, 69−83.
(10) Weston, K. D.; Carson, P. J.; Metiu, H.; Buratto, S. K. *J. Chem. Phys.* **1998**, *109*, 7474−7485.
(11) Yip, W.-T.; Hu, D.; Yu, J.; Vanden Bout, D. A.; Barbara, P. F. *J. Phys. Chem.* **1998**, *102*, 7564−7575.


**10.1021/ja030271k CCC: $25.00** 

make direct observations of the triplet state emission of single molecules.

It is well known that triplet states in solutions react very efficiently with oxygen at ambient pressures, which shortens the triplet lifetime and reduces the quantum yield of triplet emission. Therefore, the direct study of triplet states at the single molecule level can report on the collisions of individual molecules with oxygen. Quenching of phosphorescence (luminescence) is widely used to quantify molecular oxygen in various types of environments.[12−18] During the past several years, this approach has been applied to biological oxygen measurements and developed into a branch of imaging technology, broadly used for noninvasive physiological tissue oxygen measurements in both in vitro and in vivo systems.[19−22] The importance of oxygen measurements cannot be overestimated, because $O_2$ is a key component of biological energy metabolism. The ability to noninvasively and in real time assess changes in oxygenation using inexpensive optical methodology seems, therefore, very attractive. Potential clinical applications of the phosphorescence quenching technique include diagnosis and clinical evaluation of complications of diabetes, peripheral vascular diseases, cerebrovascular and cardiovascular events, eye pathology (such as diabetic retinopathy and macular degeneration), as well as detection of tumors and design of their therapeutic treatment. Quenching of phosphorescence has also been applied to biological studies on the molecular scale. For example, oxygen quenching of tryptophan[23−25] and metalloporphyrin luminescence[26] has been used to evaluate pathways of oxygen diffusion inside proteins and to look into the dynamics of oxygen channels. Therefore, the investigation of quenching processes at the single molecule level would appear to be an important and promising research avenue.

In this work, we describe single molecule measurements based on phosphorescence detection. Previous work on single molecule fluorescence has shown the effect of the interactions of the triplet states with oxygen on the fluorescence intensity.[27] Because the emitting triplet state is the lowest electronically excited state in a molecule, the direct observation of its emission presents a new perspective on the underlying photophysical and photochemical dynamics, particularly on the reactions with oxygen. By studying single molecule phosphorescence, one can assess the oxygen quenching of triplet states at the single molecule level in a direct manner. The directly obtained distributions of quenching parameters (rates) can be compared with the same distributions but obtained from ensemble measurements using inverse techniques,[28] verifying the latter and providing an insight into the mechanism of phosphorescence quenching.

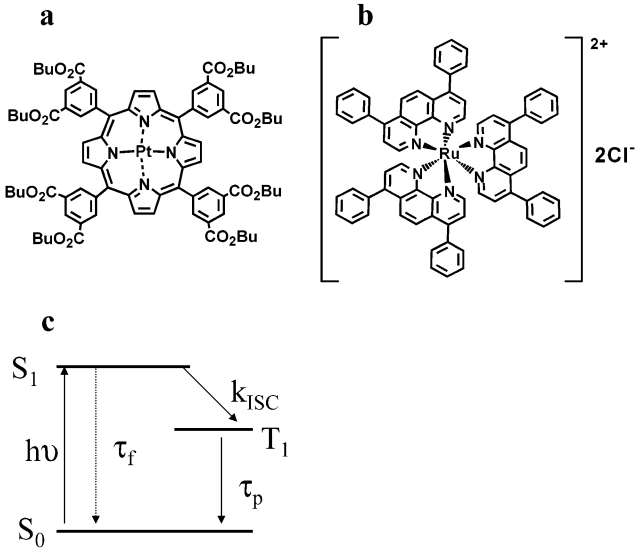


***Figure 1.*** Chemical structures of PtOBCP (a) and $Ru(dpp)_3Cl_2$ (b), and three-electronic-state model of fluorescence and phosphorescence processes.

## Materials and Methods

**Materials.** Pt octabutoxycarbonyl porphyrin (PtOBCP) and ruthenium(II)-tris-4,7-diphenyl-1,10-phenanthroline dichloride ($Ru(dpp)_3Cl_2$) (Figure 1 shows the structures) were used in the experiments.

OBCP is synthesized from the corresponding octabromoporphyrin via Pd(0)-catalyzed butoxycarbonylation reaction.[29] The Pt was inserted by refluxing the free-base porphyrin with $PtCl_2$ in benzonitrile under Ar, and the resulting complex was purified chromatographically on silica gel (Selecto) using $CH_2Cl_2$ as a solvent ($^1$H NMR ($CDCl_3$): $\delta$ 9.13 (m, 4H), 8.99 (m, 8H), 8.69 (bs, 8H), 4.44 (t, 16H, $J$ = 7 Hz), 1.78 (m, 16H), 1.46 (m, 16H), 0.94 (t, 24H, $J$ = 7.5 Hz). MALDI-TOF: $m/z$ 1609, calcd 1608.7. UV−vis (THF): $\lambda_{max}$ 403, 510, 540). PtOBCP is very soluble in many organic solvents and compatible with various polymers. The absorption and phosphorescence spectra of PtOBCP in deoxygenated DMF are shown in Figure 2. The phosphorescence lifetime of PtOBCP in deoxygenated DMF is 36 $\mu$s. The earlier reported phosphorescence lifetimes of Pt porphyrins at 77 K are in the range of 100−300 $\mu$s.[30,31]

$Ru(dpp)_3Cl_2$ (GFS Chemical, Inc.) was used as received. $Ru(dpp)_3Cl_2$ has a broad absorption spectrum in the range of 360−500 nm, peaking at ~460 nm, and emits phosphorescence at 560 nm and longer wavelengths.[32] The emission lifetime of $Ru(dpp)_3Cl_2$ in deoxygenated ethanol is 5 $\mu$s.[26]

Samples for single molecule imaging were prepared by spin casting 10 $\mu$L of PtOBCP solution (~0.1 nM, in 1% PMMA (MW: ~120 000) PRA grade dichloromethane solution, Aldrich) or $Ru(dpp)_3Cl_2$ solution (~0.1 nM, in PRA grade dichloromethane solution) onto a microscope cover slip and drying on air. Quartz cover slips (ESCO Products) were used in our experiments because they have the lowest background emission. The slips were cleaned by soaking them in a freshly prepared nochromix−concentrated sulfuric acid solution overnight, followed by rinsing them with deionized water and drying them under $N_2$.

(12) Demas, J. N.; DeGraff, B. A.; Coleman, P. B. *Anal. Chem.* **1999**, *71*, 793A−800A.
(13) Gouterman, M. *J. Chem. Educ.* **1997**, *74*, 697−702.
(14) Hartmann, P.; Ziegler, W. *Anal. Chem.* **1996**, *68*, 4512−4514.
(15) Pawlowski, M.; Wilson, D. F. *Adv. Exp. Med. Biol.* **1992**, *316*, 179.
(16) Sacksteder, L.; Demas, J. N.; DeGraff, B. A. *Anal. Chem.* **1993**, *65*, 3480−3483.
(17) Gao, Y.; Baca, A. M.; Wang, B.; Ogilby, P. R. *Macromolecules* **1994**, *27*, 7041−7048.
(18) Poulsen, L.; Ogilby, R. P. *J. Phys. Chem. A* **2000**, *104*, 2573−2580.
(19) Rumsey, W. L.; Vanderkooi, J. M.; Wilson, D. F. *Science* **1988**, *241*, 1649.
(20) Torres, I. P.; Intaglietta, M. *Am. J. Physiol.* **1993**, *265*, H1434−H1438.
(21) Vinogradov, S. A.; Lo, L.-W.; Jenkins, W. T.; Evans, S. M.; Koch, C.; Wilson, D. F. *Biophys. J.* **1996**, *70*, 1609−1617.
(22) Vanerkooi, J. M.; Maniara, G.; Green, T. J.; Wilson, D. F. *J. Biol. Chem.* **1987**, *262*, 5476.
(23) Lakowicz, J.; Weber, G. *Biochemistry* **1973**, *12*, 4161−4170.
(24) Lakowicz, J.; Weber, G. *Biochemistry* **1973**, *12*, 4171−4179.
(25) Calhoun, D.; Englander, S.; Wright, W.; Vanderkooi, J. *Biochemistry* **1988**, *27*, 8466−8484.
(26) Khajehpour, M.; Rietveld, I.; Vinogradov, S.; Prabhu, N.; Sharp, K.; Vanderkooi, J. *Proteins*: *Struct., Funct., Genet.* **2003**, in press.
(27) Hubner, C. G.; Renn, A.; Renge, I.; Wild, U. P. *J. Chem. Phys.* **2001**, *115*, 9619−9622.
(28) Vinogradov, S. A.; Fernandez-Seara, M. A.; Dupan, B. W.; Wilson, D. F. *Comp. Biochem. Physiol., A-Mol. Integr. Physiol.* **2002**, *132*, 147−152.
(29) Vinogradov, S. A.; Wilson, D. F. *Tetrahedron Lett.* **1998**, *39*, 8935−8938.
(30) Callis, J. B.; Knowles, J. M.; Gouterman, M. *J. Phys. Chem.* **1973**, *77*, 154−156.
(31) Eastwood, D.; Gouterman, M. *J. Mol. Spectrosc.* **1970**, 359−375.
(32) Murtagh, M. T.; Shahriari, M. R.; Krihak, M. *Chem. Mater.* **1998**, *10*, 3862−3869.

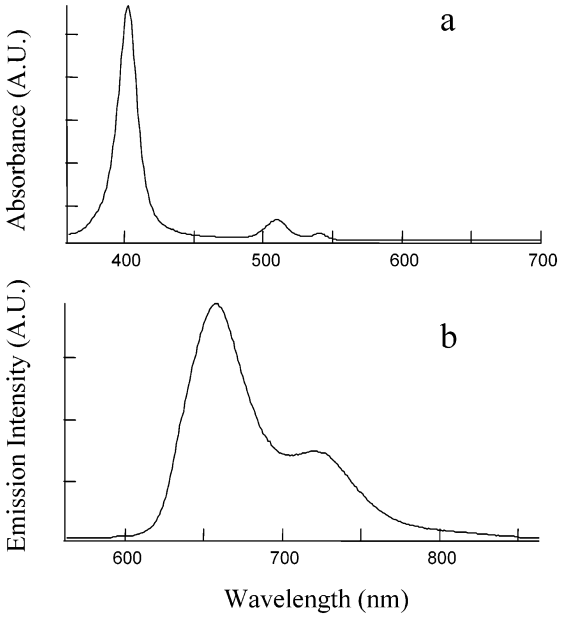


***Figure 2.*** Absorption (a) and emission (b) spectra of PtOBCP in dimethylformamide (DMF). The spectra were recorded by means of a spectrophotometer (Perkin-Elmer Lambda 35).

**Instrumentation.** The bulk phosphorescence lifetime measurements of PtOBCP in solutions and in PMMA films were performed using an earlier described system.[27] The confocal microscope equipped with a scannable stage used in this work has been described previously.[33] Briefly, the sample scanning stage incorporates a closed-loop X,Y feedback for accurate determination of the location of each molecule in the imaging experiments. The sample is mounted on the scanning stage and excited by a laser. An objective (1.3 N.A.) is used to produce a nearly diffraction-limited focused laser spot on the sample and to collect phosphorescence emitted by the molecules. A combination of filters was used to isolate the phosphorescence from the excitation laser and background signal. By raster scanning the sample, one can obtain single molecule phosphorescence images. Each molecule could be studied by centering it in the laser focus and detecting its individual phosphorescence signal. A liquid nitrogen cooled CCD array detector (Roper Scientific) and an associated imaging spectrograph (Acton Research) were coupled to the microscope and used to record the phosphorescence spectra of the sample. The 514.4 nm line and 457.9 nm line from an Ar ion laser were employed for excitation of PtOBCP and $Ru(dpp)_3Cl_2$, respectively. An inverted glass funnel was connected to gas tanks with $N_2$, Ar, and $O_2$ (BOC gases, Inc., 99.99% purity) and attached to the microscope stage to cover the samples to control $O_2$ partial pressures above the PMMA films. A system with multiple inlets and flow meters allowed gas mixtures to be varied in desired proportions.

## Results

The single molecules of PtOBCP and $Ru(dpp)_3Cl_2$ deposited respectively into PMMA thin film and onto a quartz surface exhibited phosphorescence spectra on repetitive excitation (Figure 3) that were very similar to those obtained from bulk experiments. Figure 4 shows the images of some $Ru(dpp)_3Cl_2$ single molecules on a quartz surface exposed to different argon/air mixtures at 1 atm. Single molecule images of PtOBCP on quartz surfaces also showed sensitivity to oxygen content in gas mixtures. The results shown in Figure 4 clearly indicate that the mean phosphorescence signal of each of the molecules

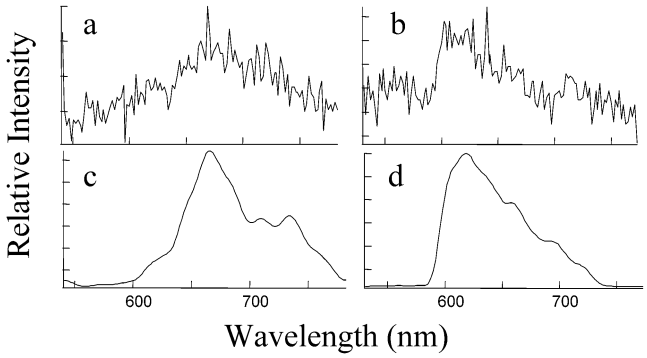


***Figure 3.*** Spectra of a single molecule of PtOBCP in PMMA (a) and single molecule of $Ru(dpp)_3Cl_2$ (b) on quartz surface. The spectra of bulk PtOBCP in PMMA and bulk $Ru(dpp)_3Cl_2$ on quartz surface are shown in (c) and (d). The bulk spectra were recorded using the CCD array detector setup mentioned in the text, with the same interference filters and dichroic reflectors as were used in single molecule experiments but with higher sample concentration.

in these images is reduced by the presence of oxygen; that is, it is clear that the triplet states are being quenched by oxygen.

In the experiments, bright single molecules were first located under a pure argon (or nitrogen) atmosphere, and then the gas mixture was changed and additional images were recorded. Figure 5 shows representative phosphorescence intensity−time records in pure argon for single PtOBCP and $Ru(dpp)_3Cl_2$, respectively. The single step photobleaching, evident in the figures, clearly indicates that the signals originate from single molecules. Figure 6 shows two typical intensity−time records of $Ru(dpp)_3Cl_2$, obtained using 1% $O_2$ in an Ar mixture, and also displays a single molecule intensity−time record of $Ru(dpp)_3Cl_2$ and the effect of changing the gas composition during the record. As shown in Figure 6c, during the first 20 s, photons were collected from a molecule in an atmosphere containing 1% $O_2$. At ∼20 s into the record, the mixed gas was replaced by pure Ar, and a significant increase in the phosphorescence intensity is seen in the subsequent part of the record (between ∼20 and 55 s). Experiments of this type were qualitatively reproducible in the sense that there was always an increase in the single molecule signal when oxygen was removed.

The quenching constants of single molecules were calculated on the basis of a Stern−Volmer relation (see eq 1) by using total relative phosphorescence intensities of single molecules collected from single molecules images. Figure 4 shows examples of a typical set of images obtained at three different oxygen concentrations (respectively at ∼0% (pure Ar), 0.5%, and 3 vol %). Comparable images obtained at four different oxygen concentrations (respectively at ∼0% (pure Ar), 0.5%, 1%, and 3 vol %) provided the four points of inverse relative intensity versus oxygen concentration (Stern−Volmer plot) for each molecule, which were fitted by the method of least squares to a straight line. Figure 7 shows three typical Stern−Volmer plots of inverse relative phosphorescence intensity versus oxygen pressure for three single $Ru(dpp)_3Cl_2$ molecules on a quartz surface. The slope of the line was used to represent the quenching constant for each molecule as discussed below. Figure 8 shows the distribution of the quenching constants, derived from such measurements for 377 individual molecules.

The count rate obtained for PtOBCP was ∼1000 counts/s, and for $Ru(dpp)_3Cl_2$ it was ∼2000 counts/s as shown in Figure 5. This count rate is lower, by at least 10 times, than

(33) Bopp, M. A.; Sytnik, A.; Howard, T. D.; Cogdell, R. J.; Hochstrasser, R. M. *Proc. Natl. Acad. Sci. U.S.A.* **1999**, *96*, 11271−11276.

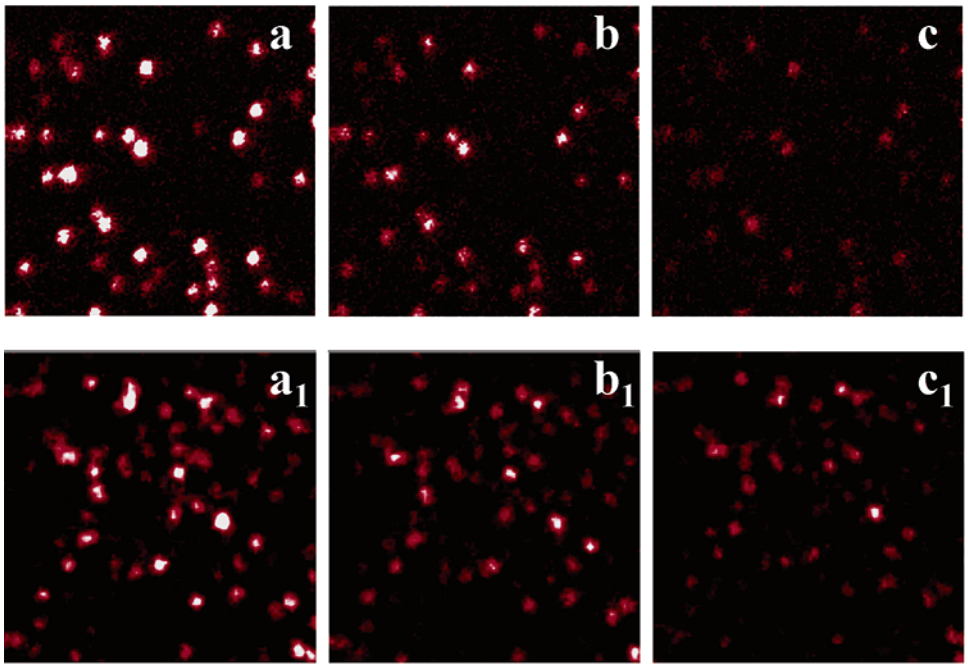


***Figure 4.*** Single molecule phosphorescence images of $Ru(dpp)_3Cl_2$ immobilized on a quartz surface in pure Ar (a and $a_1$), in Ar with 0.5% $O_2$ (b and $b_1$), and in Ar with 3% $O_2$ (c) and $c_1$). The two sets of three images were obtained from two different regions of the sample.

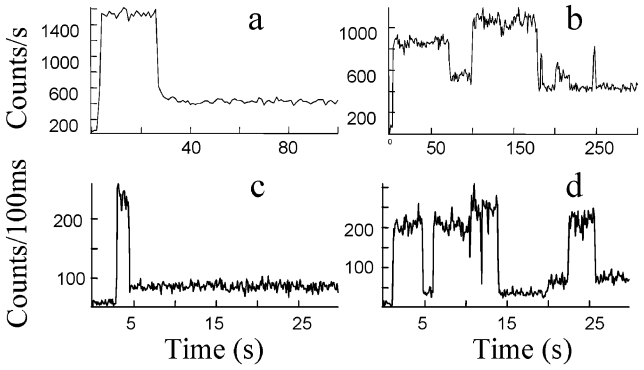


***Figure 5.*** Typical time intensity records of phosphorescence of single PtOBCP molecules in PMMA (a, b), and of single $Ru(dpp)_3Cl_2$ molecules on a quartz surface (c, d). Data were collected in pure $N_2$. The data in (a) and (b) are binned in one-second intervals, while the data in (c) and (d) are binned in 100 ms intervals.

conventional single molecule fluorescence signals. The background signal in these experiments is ~400 counts/s.

## Discussion

The limiting features of single molecule phosphorescence are different from those of fluorescence. As sketched in Figure 1c, the triplet state is reached by intersystem crossing from the lowest singlet state, which is ascribed an observed lifetime of $\tau_f$. The efficiency of triplet formation is $\tau_f k_{ISC}$, where $k_{ISC}$ is the rate coefficient for intersystem crossing. In the present examples, this efficiency is close to unity, and $\tau_f$ is in the picosecond domain. Thus, the fluorescence signals from these molecules are too small to observe at the single molecule level. On the other hand, the singlet excited state could be revisited with a specific rate as large as $k_{ISC} \times \exp[-\Delta E/k_B T]$, where $\Delta E$ is the singlet−triplet energy gap. For an intersystem crossing rate constant of $10^{11}$ $s^{-1}$, 300 K, and the gap of 5000 $cm^{-1}$,[34,35]

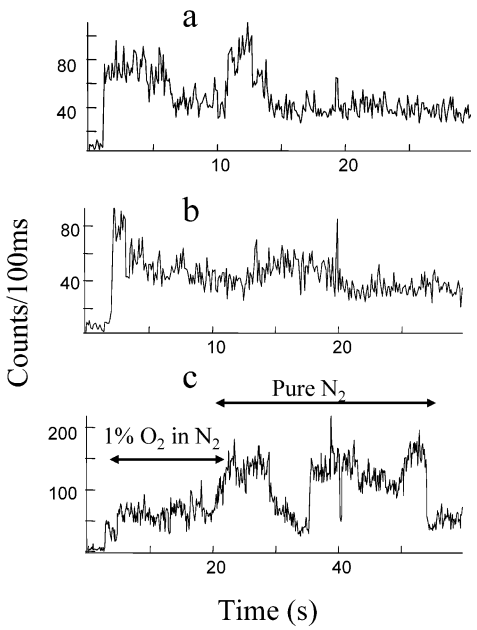


***Figure 6.*** Typical time intensity records of the transient phosphorescence intensities of single $Ru(dpp)_3Cl_2$ molecules on a quartz surface in the presence of $O_2$. In (a) and (b), data were collected in Ar mixed with 1% $O_2$. In the first part of (c), from ~3−20 s the ambient gas is $N_2$ mixed with 1% $O_2$; beyond ~20 s the ambient gas is pure $N_2$.

the singlet state would seldom be revisited during the lifetime of the triplet state (ca. 10 $\mu$s). In the absence of recrossing to the singlet state, the emissive triplet can undergo either spontaneous emission, internal conversion to the ground electronic state, energy transfer, or chemistry, including electron transfer. Therefore, our expectations are that the phosphorescence intensity−time records of single molecules will be different from fluorescence records. The low count rate in

(34) Watts, R. J.; Crosby, G. A. *J. Am. Chem. Soc.* **1971**, *93*, 3184−3188.

(35) Sauvage, J.-P.; Collin, J.-P.; Chambron, J.-C.; Guillerez, S.; Coudret, C.; Balxani, V.; Barigelletti, F.; Cola, L. D.; Flamigni, L. *Chem. Rev.* **1994**, *94*, 993−1019.

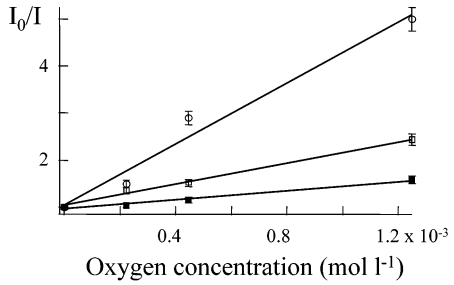


***Figure 7.*** Typical Stern−Volmer plots of oxygen quenching of phosphorescence for three single $Ru(dpp)_3Cl_2$ molecules on a quartz surface. The linear fits correspond to slopes of 3246, 1119, and 484 L $mol^{-1}$, respectively.

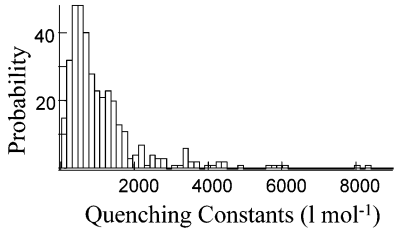


***Figure 8.*** Distribution of quenching constants as defined in the text, of 377 single molecules of $Ru(dpp)_3Cl_2$ on a quartz surface.

comparison with fluorescence originates in relatively long triplet lifetimes, which limit the rate at which molecules can be excited. For example, with a triplet lifetime of 36 $\mu$s, a molecule returns to the ground for re-excitation at a maximum rate of only $2.8 \times 10^4$ times per second, no matter how high the excitation intensity is. In contrast, high quantum yield fluorescent molecules having low probability of intersystem crossing are not normally close to saturation at many millions of excitations per second.

**Single Molecule Phosphorescence Quenching by Molecular Oxygen.** The expectations for the effects of oxygen collisions are quite different for the two types of experiments carried out in this work. The $Ru(dpp)_3Cl_2$ molecules were spin coated onto a fused quartz surface with dichloromethane and expected to be incorporated in a thin film of surface bound water and solvent.[36] This picture is confirmed by the experiments discussed below. The PtOBCP sample is deposited in a PMMA film so that the effective time scale for oxygen interactions is controlled by the solubility and diffusion constant of oxygen in PMMA.

Over a wide range of concentrations in bulk solutions, the relationship between the oxygen concentration, $n_{O_2}$, in the neighborhood of the triplet state emitter, the triplet lifetime $\tau$, and phosphorescence intensity $I$ is usually described by the Stern−Volmer relationship:

$$I_0/I = \tau_0/\tau = \tau_0(1/\tau_0 + k_2 n_{o_2}) = 1 + K_Q n_{o_2} \qquad (1)$$

where $I_0$ and $\tau_0$ are the intensity and the phosphorescence lifetime in the absence of $O_2$, $k_2$ (concentration$^{-1}$ $s^{-1}$) is the bimolecular rate constant, and $K_Q$ (concentration$^{-1}$) is a related constant describing the kinetics of quenching. In the literature, the "quenching constant" is often defined from the expression $(\tau_0 - \tau)/\tau_0\tau = k^* \times n_{O_2}$, where $k^* = K_Q/\tau_0$. The quenching constants depend on the diffusion of $O_2$ to the phosphorescent center and on the mechanism of quenching within the encounter complex. It is usually considered that quenching occurs via a short-range energy exchange, resulting in the production of singlet oxygen $O_2^{\uparrow}$. In bulk experiments, the average intensities and lifetimes in the presence and absence of $O_2$ determine the ensemble averaged quenching rate coefficient. Establishing a molecular level description of the oxygen quenching mechanism from bulk experiments in inhomogeneous media, even those that are time resolved,[37−39] is not a straightforward task. There is uncertainty in the $O_2$ mobility in the microenvironments where phosphors are located and in determining experimentally the distributions of the microscopic rates of reaction between the triplet and $O_2$. In the simplest theory of quenching, $K_Q$ is given by the product of the excited-state lifetime $\tau_0$ and a bimolecular rate constant $k_2$. The mean distance traveled by an oxygen molecule in a time period $t$ is $(2Dt)^{1/2}$, where $D$ is the diffusion coefficient of oxygen in the medium. If this distance is very much greater than the effective radius, $R$, of the molecule whose phosphorescence is being quenched, the quenching rate constant is expected to be time independent and the Schmolukowski limit of quenching where $k_2 = 4\pi RD$ is expected to be valid. The diffusion constant for oxygen in PMMA is in the range $10^{-8}$ $cm^2$ $s^{-1}$,[18] so $R$ is approximately 1 nm and $(2Dt)^{1/2}$ is larger than $R$ for times in excess of $\sim$0.5 $\mu$s. Our experiments are on the millisecond time scale during which time oxygen molecules mostly probably diffuse more than 44 nm.

Normally, eq 1, as a relationship describing the bulk response, assumes that the average distribution of oxygen molecules around the emitting centers is not influenced by the previous quenching event, so $n_{O_2}$ is simply the mean concentration of oxygen. In a single molecule experiment, where the same molecule is excited repetitively, a key parameter becomes the time separation between the successive excitations. The lifetime of the quenching reaction product, for example singlet oxygen, is in the range of tens of microseconds,[40] so we are not concerned about the pulse-induced depletion of the quencher in the experiments reported here.

**Single Molecules of $Ru(dpp)_3Cl_2$.** We first consider the experiments with $Ru(dpp)_3Cl_2$. In these experiments, individual quenching events could be measured, which in principle permits experimental evaluation of the distributions of quenching constants that are hidden from ensemble average measurements. For each molecule, the signal is measured in the absence of oxygen and at known ambient oxygen concentrations. The sample is continually purged with gas mixtures that are in contact with the surface. Although the molecules are surface bound, they are definitely dissolved in a solvent layer on the surface. This is clear from a simple estimation of the total number of $O_2$ molecules crossing the surface of an immobilized hemisphere having the radius $R$ of the molecule per second. The diffusion equation yields the value $1/\tau = 2\pi RDN$ for this rate, and the corresponding rate of quenching is between $1/\tau$ and $1/(9\tau)$. $D$ is the oxygen diffusion coefficient, and $N$ is the oxygen number density. The factor of $^1/_9$ accounts for the fraction of collision pairs that have the zero electron spin needed for quenching to take place.[39] For the full factor of $^1/_9$ to be

(36) Froehlich, F. F.; Milster, T. D. *Appl. Phys. Lett.* **1997**, *70*, 1500−1502.
(37) Draxler, S.; Lippitsch, M. E.; Klimant, I.; Kraus, H.; Wolfbeis, O. S. *J. Phys. Chem.* **1995**, *99*, 3162−3167.
(38) Zhang, X.; Rodgers, M. A. J. *J. Phys. Chem.* **1995**, *99*, 12797−12803.
(39) Abdel-Shafi, A. A.; Beer, P. D.; Mortimer, R. J.; Wilkinson, F. *J. Phys. Chem.* **2000**, *104*, 192−202.
(40) Okamoto, M.; Tanaka, F.; Teranishi, H. *J. Phys. Chem.* **1990**, *94*, 669−672.

incorporated, the electron spin must be a good quantum number. The spin prohibition lessens as the metal atomic number increases. If the gaseous diffusion coefficient of $O_2$ in Ar at STP is $D = 0.0181$ cm$^2$ s$^{-1}$ and $R = 1$ nm, the value of $1/\tau$ for 1% $O_2$ in Ar at 1 atm is $3.1 \times 10^9$ s$^{-1}$, and for 99.99% Ar, in which the main impurity is $O_2$, the value is $3.1 \times 10^7$ s$^{-1}$. The triplet lifetime for $Ru(dpp)_3Cl_2$ is 5 $\mu$s in the absence of oxygen, so if each of these collisions were to quench the phosphorescence, the single molecule signal should have been extremely weak and barely observable. Because this is not the case, this calculation confirms that the surface bound molecules are not freely accessible to oxygen from the ambient gas. Angular constraints in the $O_2/Ru(dpp)_3Cl_2$ reaction coordinate cannot account for this discrepancy of the quenching probability. If oxygen molecules needed to approach $Ru(dpp)_3Cl_2$ within a cone of latitude $\theta$ to quench the triplet state at the observed rates, the effective collision frequency would be decreased by a factor $(1 - \cos\theta)/2$. The angle $\theta$ would be required, in this case, to be in the range of just a few degrees to account for the experimentally observed slow quenching. Such a constraint is totally inconsistent with bulk quenching measurements, which suggest that the quenching is diffusion controlled.[39] From the analysis in the previous paragraph, we assert that for each $Ru(dpp)_3Cl_2$ molecule we can define an oxygen free phosphorescence lifetime $\tau_0$ and a bimolecular rate constant $k_2$. It is important to note that in the present work the linearity of the Stern−Volmer plot is assumed. We have collected only four points per molecule, and this is insufficient to establish confidently whether the relationship (1) is valid over the range of pressures that were studied. However, the approach is clearly reasonable, and the linear fits have standard deviations that are on average 252 L mol$^{-1}$.

The sample is heterogeneous so there may be a distribution of material (e.g., density, structure) leading to a distribution of effective oxygen concentration and a distribution of diffusion constants in the surface solvent layer. We assume that Henry's law holds for each region of this distribution so that the concentration of oxygen is proportional to the ambient gas-phase oxygen concentration and $\alpha$ is the proportionality parameter, that is, the solubility coefficient, which characterizes the distribution. Thus, the slope of the plot of the intensity ratio versus ambient oxygen pressure for a given molecule characterizes the product $\alpha\tau_0k_2$ for each molecule and its surroundings. The distribution function of quenching constants shown in Figure 8, obtained from the measurements performed on many molecules, is a distribution of these products. The mean quenching constant is $K_Q = 1119$ L mol$^{-1}$ or $k_2 = 2.24 \times 10^8$ L mol$^{-1}$ s$^{-1}$. The first and second moments of this distribution are $\langle\alpha\tau_0k_2\rangle$ and $\langle(\alpha\tau_0k_2 - \langle\alpha\tau_0k_2\rangle)^2\rangle$. While there are known variations of radiative lifetimes for surface bound molecules, these have relatively small variances as compared with what we observe, so we will assume that they do not contribute much to the measured distributions. This assumption could be evaluated by measurements of the single molecule phosphorescence lifetimes, but we have no way to accomplish such an experiment at present. On the basis of this assumption, the Schmolukowski limit of quenching and a fixed value of 1 nm for $R$, the experiment yields the mean and the standard deviation of the $\alpha D$ distribution as: $\langle aD\rangle = 3.0 \times 10^{-7}$ cm$^2$ s$^{-1}$ and $\langle(\alpha D - \langle aD\rangle)^2\rangle^{1/2} = 3.2 \times 10^{-7}$ cm$^2$ s$^{-1}$. The distribution function is not well fit by a Gaussian and is clearly stretched out to larger quenching constants. This suggests that there is a range of accessibilities to oxygen that is very likely related to the distance distribution of $Ru(dpp)_3Cl_2$ molecules from the surface of the film. The quenching rate constants for similar Ru(II) complexes[41] in solutions are in the range $2.2-4.2 \times 10^9$ L mol$^{-1}$ s$^{-1}$. Thus, it appears that on average the solubility factor for $Ru(dpp)_3Cl_2$ in the surface solvent layer of quartz is about 0.1, which is very similar to the expectations for solutions.

**Single Molecules of PtOBCP.** The signal-to-background ratios in the experiments involving PtOBCP were considerably lower than those for the Ru complex, so the data are less extensive. Nevertheless, we have definitively shown that the triplet to singlet emission of this Pt porphyrin can be used as a single molecule detector. This result may be very useful for the study of heme protein dynamics because these molecules can be incorporated into proteins. We were able to estimate the quenching constants for a few molecules, typified by the images in Figure 4, and obtain an average value of $K_Q = 100$ L mol$^{-1}$ corresponding to the value of $k_2 = 2.8 \times 10^6$ L mol$^{-1}$ s$^{-1}$. The quenching constant for this porphyrin was also measured in a bulk PMMA sample using previously described methods[42,43] and was found to be 129 mmHg$^{-1}$ s$^{-1}$, with the reference to the ambient gas pressure. If Henry's law is assumed, this implies $k_2 = 2.4 \times 10^6$ L mol$^{-1}$ s$^{-1}$, which is very close to the value found from the single molecule measurements. If $R$ is chosen as 1 nm, the bulk measurement gives a value for $\langle aD\rangle$ of about $3.2 \times 10^{-9}$ cm$^2$ s$^{-1}$, to be compared with the value of $3.7 \times 10^{-9}$ cm$^2$ s$^{-1}$ from the single molecule experiments, assuming the distribution of triplet lifetimes in the absence of oxygen to be narrow. Taking the solubility of oxygen in PMMA to be $\sim 8.7 \times 10^{-3}$ M/atm,[44] we calculated the value of $D$ for oxygen in PMMA to be $1.5 \times 10^{-8}$ cm$^2$ s$^{-1}$ from our bulk measurements and $1.8 \times 10^{-8}$ cm$^2$ s$^{-1}$ from the single molecule experiments. Both values are in reasonable agreement with the data obtained by Charlesworth[45] ($D = 1.4 \times 10^{-8}$ cm$^2$ s$^{-1}$) and by Kaptan[46] ($1.9 \times 10^{-8}$ cm$^2$ s$^{-1}$ (20 °C)) but are somewhat lower than the recent results of Ogilby[18] ($4.3 \times 10^{-8}$ cm$^2$ s$^{-1}$) and other groups ($3.8 \times 10^{-8}$ cm$^2$ s$^{-1}$,[47] $3.7 \times 10^{-8}$ cm$^2$ s$^{-1}$,[48] $3.3 \times 10^{-8}$ cm$^2$ s$^{-1}$ [49]). When the small variations in temperature, film thickness, density, and quenchable dye among these various experiments are considered, the single molecule average can be considered to be consistent with documented bulk measurements of the diffusion coefficient of oxygen in PMMA.

The data in Figure 5a,b give information about the photostability of the triplet state of PtOBCP in PMMA. In the intensity time records (Figure 5a), the triplet signal remains steady for about 20 s, which corresponds to about 23 000 counts. There are no significant fluctuations of this signal on time scales longer

(41) Garcia-Fresnadillo, D.; Georgiadou, Y.; Orllana, G.; Braun, A. M.; Oliveros, E. *Helv. Chim. Acta* **1996**, *79*, 1222−1238.
(42) Rozhkov, V.; Wilson, D.; Vinogradov, S. *Macromolecules* **2002**, *35*, 1991−1993.
(43) Vinogradov, S. A.; Fernandez-Searra, M. A.; Dugan, B. W.; Wilson, D. F. *Rev. Sci. Instrum.* **2001**, *72*, 3396−3406.
(44) Perterson, C. M. *J. Polym. Sci.* **1968**, *12*, 2649−2667.
(45) Charlesworth, J. M.; Gan, T. H. *J. Phys. Chem.* **1996**, *100*, 14922−14927.
(46) Kaptan, H. Y. *J. Appl. Polym. Sci.* **1999**, *71*, 1203−1207.
(47) MacCallum, J. R.; Rudkin, A. L. *Eur. Polym. J.* **1978**, *14*, 655−656.
(48) Kaptan, Y.; Pekcan, O.; Arca, E.; Guven, O. *J. Appl. Polym. Sci.* **1989**, *37*, 2577−2585.
(49) Higashide, F.; Omata, K.; Nozawa, Y.; Yoshioka, H. *J. Polym. Sci., Polym. Chem. Ed.* **1977**, *15*, 2019−2028.

than a 1 s integration period. In every case, photobleaching ultimately terminates the intensity time record.

**Unusual Intensity Jumps.** Normally, in single molecule fluorescence experiments, it is very common to observe fluorescence signals that undergo intensity jumps on time scales that are long as compared with photophysical parameters. Figure 5b,d and Figure 6 evidence the occurrence of states having no emission on a variety of time scales not seen in conventional photophysics, ranging from fractions of a second to tens of seconds. Sudden changes in the orientation of the molecular transition dipoles can affect the overall emission signal, but certainly the PtOBCP is essentially immobilized in PMMA. Further evidence that these dark states are not caused by reorientation is provided by the circular symmetry of PtOBCP, which ensures that its emission can never be extinguished by reorientation. This situation should also be the case for $Ru(dpp)_3Cl_2$, based on its emission anisotropy.[50] Clearly, these dark states represent chemical transformations or rearrangements of molecules that produce nonemissive states. This chemistry could involve oxygen, the polymer matrix, or both of these. One possible explanation, based on the high sensitivity of the phosphorescence signals to oxygen, is that during the dark periods an oxygen molecule is trapped near the emitter. The lifetime of singlet oxygen in PMMA is 35 $\mu$s,[51] so if it was trapped after formation by the energy transfer from the triplet state it would relax quickly enough to have ground-state $O_2$ present when the next photon was absorbed. However, for this explanation to be correct, the $O_2$ molecules would need to be trapped near the chromophores for many seconds, whereas for normal diffusional motion the residence time of $O_2$ in a 1 nm radius sphere is in the submicrosecond range, even for the case of PMMA. To provide such long trapping times, the barrier to escape of the trapped molecules would be required to be in excess of 10 kcal/mol, which appears to be too large for any physical interaction between oxygen molecules and the emitters. Therefore, a more likely explanation involving oxygen is that sometimes singlet oxygen is unable to escape from the neighborhood of the chromophore before it undergoes a chemical reaction to produce a product or products that reversibly re-form the unmodified emitter. One possibility is the formation of a long-lived Pt porphyrin cation-radical. The involvement of cation radicals of chlorophylls was suggested previously for the occurrence of dark states of single molecules of light-harvesting complexes, LH2.[52] Furthermore, it has been shown that ZnTPP cation-radicals can survive in some confined molecular environments for minutes.[53] Dark states also occur when the oxygen pressure is very low, so it is quite likely that the triplet states react with the matrix in electron-transfer processes to produce cation-radicals. The rates of electron transfer are extremely slow and are difficult to pin down from the present data. In future work, by acquiring many more intensity time records it should be possible to characterize the correlations between the dark state occurrences and the oxygen pressure. We have not been able to establish with certainty on the basis of available data whether the recovery of the phosphorescence signal from the dark states after many seconds is a thermal or photoinduced process.

**Single Molecule Oxygen Sensor.** Ultrasmall sensors are crucial for precise intracellular/subcellular analyte detection. Small sensor size provides many advantages, such as greater chemical imaging resolution and acuity, low absolute detection limit, and faster response. So far, the smallest sensors that have been developed include micro and ultramicro electrodes[54−57] and optical nanosensors.[58−60] Oxygen is a key substance in biological systems and is either produced by autotrophic photosynthesis in the presence of light or consumed by different metabolic processes. Knowledge of oxygen concentration/gradients in biological samples is of paramount importance for the understanding and quantification of these processes. In medical and biochemical research, or even in clinical applications, there is a need to measure oxygen concentrations in living cells or tissues with high spatial resolution and also noninvasively. Therefore, a single molecule oxygen sensor could prove very useful. In principle, it offers minimum sensor size, minimizes the perturbation of the sample, and gives the opportunity for optimum spatial resolution.

The results shown in Figures 4−7 clearly demonstrate the proof of principle for a single molecule oxygen sensor which could be configured to measure ultrasmall oxygen concentrations or even the presence of a single oxygen molecule in a particular spatial region. PtOBCP and $Ru(dpp)_3Cl_2$ are both quite soluble in many organic solvents and compatible with various polymers, so they already could be used as single molecule oxygen sensors to probe oxygen diffusion rates in small volumes of polymers. To apply this technique to biological systems, the phosphor would be required to be water soluble, but this does not appear to pose any fundamental difficulty, and, in fact, such phosphors are currently being developed.[42,61] The background signal in the experiments is mostly from the scatter, which has lifetime at the nanosecond level. So, in principle, when time gating methods were employed, the background counts could be significantly reduced and the sensitivity to oxygen could be increased.

**Acknowledgment.** This work was supported by NIH grant GM 48130 using instrumentation developed by the NIH Research Resource grant NIH P41 RR001348.

JA030271K

(50) Degraff, B. A.; Demas, J. N. *J. Phys. Chem.* **1994**, *98*, 12478−12480.
(51) Schiller, K.; Mueller, F.; Werner. *Polym. Int.* **1991**, *25*, 19−22.
(52) Bopp, M. A.; Jia, Y. W.; Li, L. Q.; Cogdell, R. J.; Hochstrasser, R. M. *Proc. Natl. Acad. Sci. U.S.A.* **1997**, *94*, 10630−10635.
(53) Morishima, Y.; Aota, H.; Saegusa, K.; Kamachi, M. *Macromolecules* **1996**, *29*, 6505−6509.
(54) Avnir, D.; Braun, S.; Lev, O.; Levy, D.; Ottolenghi, M. In *Sol−Gel Optics Processing and Applications*; Klein, L. C., Ed.; Kluwer Academic Publications: Norwell, MA, 1994; pp 539−582.
(55) Lau, Y. Y.; Abe, T.; Ewing, A. G. *Anal. Chem.* **1992**, *64*, 1702−1705.
(56) Meulemans, A.; Poulain, B.; Baux, G.; Tauc, L.; Henzel, D. *Anal. Chem.* **1986**, *58*, 2088−2091.
(57) Cui, Y.; Wei, Q.; Park, H.; Lieber, C. M. *Science* (*Washington, DC*) **2001**, *293*, 1289−1292.
(58) Clark, H. A.; Kopelman, R.; Tjalkens, R.; Philbert, M. A. *Anal. Chem.* **1999**, *71*, 4837−4843.
(59) Xu, H.; Aylott, J. W.; Kopelman, R.; Miller, T. J.; Philbert, M. A. *Anal. Chem.* **2001**, *73*, 4124−4133.
(60) Brasuel, M.; Kopelman, R.; Miller, T. J.; Tjalkens, R.; Philbert, M. A. *Anal. Chem.* **2001**, *73*, 2221−2228.
(61) Rietveld, I.; Kim, E.; Vinogradov, S. *Tetrahedron* **2003**, *59*, 3821−3831.